

A Novel Paradigm of Polarization Reconfigurable NOMA with Dynamic Ordered SIC

Thong Ngo, Julio Acevedo, Paul Oh, Hen-Geul Yeh[†] and Sean Kwon[†]
Department of Electrical Engineering, California State University, Long Beach
Email: {thong.ngo, julio.acevedo01, paul.oh}@student.csulb.edu
[†]{henry.yeh, sean.kwon}@csulb.edu

Abstract—A new paradigm in non-orthogonal multiple access (NOMA) is proposed and yields significant improvement of sum and individual channel capacity in this paper. Both near and far users can fulfill successive interference cancellation (SIC) in the proposed scheme; while conventional NOMA cannot fulfill SIC at the far user. The proposed scheme of *dynamic ordered SIC* in this paper utilizes polarization reconfigurable antennas at the transmitter (Tx) and receiver (Rx), which is denominated *polarization reconfigurable NOMA (PR-NOMA)*. Furthermore, PR-NOMA can apply SIC for both users with the same signal-to-noise ratio (SNR). Comprehensive simulation results validate that the novel paradigm of PR-NOMA remarkably outperforms the conventional NOMA with more than 3 bits/sec/Hz improvement in sum channel capacity in the scenario that two users have the same SNR.

I. INTRODUCTION

The 6th generation (6G) and future wireless communication systems require extremely high data rate and spectrum efficiency. With this motivation, non-orthogonal multiple access (NOMA) has been regarded as a promising multiple access scheme to further increase the spectral efficiency beyond the conventional orthogonal multiple access (OMA) schemes [1]–[4]. In addition to conventional time, frequency, space and code division multiple access schemes, NOMA utilizes the power domain to maximize the sum channel capacity in the aid of successive interference cancellation (SIC).

It is reported that adopting NOMA in the communication system outperforms the conventional system with orthogonal multiple access (OMA) schemes in terms of spectral efficiency and the outage probability [2], [5]. Fixed or dynamic power allocation schemes are used within NOMA systems depending on the available feedback type of channel state information (CSI). For instance, it is reported that a fixed power allocation scheme of NOMA can achieve higher sum rates than OMA in the high SNR regime, in particular, in the scenario that users have disparate channel conditions [6]. Extensive research has been conducted to explore optimal power allocation techniques in NOMA systems. Consequently, a range of solutions has been proposed, considering various metrics such as energy efficiency, sum rate, and symbol error rate [7]–[11]. Arbitrary number of users are considered in several research works;

This work was supported financially by The Aerospace Corporation (G255621100).

Thong Ngo, Julio Acevedo, Paul Seungcheol Oh and Sean Kwon are co-first authors with the equal contribution; Sean Kwon is the corresponding author.

whereas, it is prevalent to take into account the scenario of the dual-user NOMA due to the issue of the complexity.

The decoding order of SIC in NOMA is determined based on channel state information (CSI) estimated at the receiver (Rx) of each user. In conventional NOMA, the higher transmission power is allocated to the signal of the user with the longer distance or lower channel gain. Consequently, the desired signal of the far user has higher received signal power than the desired signal of the near user at the receivers of both near and far users. For this reason, the near user can apply SIC to eliminate the interfering signal, which is the desired signal of the far user, and subsequently decode its desired signal. Meanwhile, the far user cannot apply SIC, but directly decodes its desired signal while accounting for the interfering signal caused by the desired signal of the near user. In contrast, it is noteworthy that the novel paradigm of *polarization reconfigurable NOMA (PR-NOMA)* proposed in this paper enables the NOMA system to apply SIC at not only the near user but also the far user as it will be demonstrated in detail.

PR-NOMA utilizing polarization reconfigurable antennas can realize the required reception power ratio between two or more signals for the achievement of the satisfactory performance of SIC in NOMA. Furthermore, not only the near user but also the far user can apply SIC in decoding the desired signal via dynamically changing the decoding order in SIC. The polarization domain has attracted substantial attention, and interesting research has recently been reported in several aspects of utilizing it [12]–[19]. Utilizing characteristics of polarization/depolarization has shown large potential to increase channel capacity and spectral efficiency; and to reduce bit/symbol error rate (BER/SER) [13], [17], [20]–[22]

This paper utilizes polarization for a new scheme of NOMA.

The primary contributions of this paper can be summarized as follows:

- we propose a new paradigm of *PR-NOMA* utilizing polarization reconfigurable antennas to superimpose signals designated for the near and far users, yielding remarkable benefit in sum/individual channel capacity;
- we propose *dynamic ordered SIC* where both the near and far users can apply SIC for the superimposed signal and eliminate the interfering signal via swapping the order of received signal power;
- comprehensive simulation results are provided to validate the feasibility of dynamic ordered SIC and significant im-

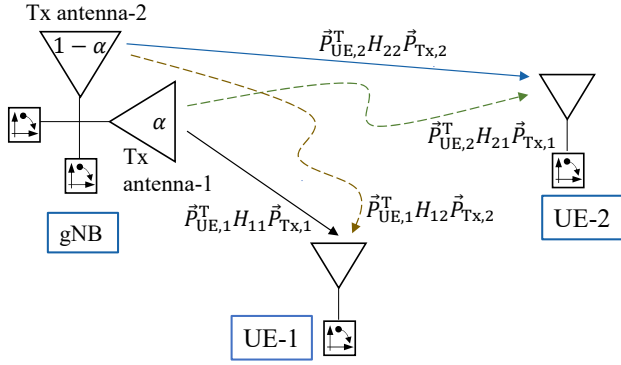


Fig. 1. PR-NOMA downlink communication system model.

provement of channel capacity beyond the conventional NOMA;

- detailed empirical analysis on the behavior of PR-NOMA is presented. The analysis includes the distribution of the transmission power allocation coefficient and the success rate of dynamic ordered SIC to foster successful SIC at both the near and far users.

The remainder of this paper is as follows. Section II presents the PR-NOMA system model focusing on the effective channel coefficient matrix with polarization reconfigurable antennas. In Section III, a novel scheme of dynamic ordered SIC is proposed, and theoretical analysis and derivation of sum/individual channel capacity are described in detail. The superiority of PR-NOMA in channel capacity is validated, and unique characteristics of PR-NOMA is demonstrated in Section IV. Finally, Section V concludes the paper.

II. SYSTEM MODEL

The proposed PR-NOMA system is illustrated in Fig. 1. The next-generation Node B (gNB) including the conventional base station (BS) utilizes two polarization reconfigurable antennas; and each of the first and second user equipments, i.e., UE-1 and UE-2 has a single polarization reconfigurable antenna. The gNB polarization vector $\vec{p}_{Tx,j}$ with $j \in \{1, 2\}$ and UE polarization vector $\vec{p}_{UE,i}$, with $i \in \{1, 2\}$ are configured by the gNB and UEs, respectively, according to the channel state information (CSI). We assume that perfect CSI at all antenna elements is feasible at the Rx (CSIR) as well as the Tx (CSIT). Note that the CSI is available for both orthogonal polarization directions; it can be obtained through training schemes analogous to those employed in antenna selection systems [13], [23]. The impact of imperfect CSI is outside the scope of this paper and will be analyzed in future work.

In comparison to conventional NOMA, the novel PR-NOMA scheme utilizes two polarization-reconfigurable transmission antenna elements with the same total transmission power, so that the signals designated for UE-1 and UE-2 are superimposed with different polarization. It is worth mentioning that the PR-NOMA system model is reasonable and feasible considering numerous antenna elements supported by

ultra-massive multiple-input multiple-output (MIMO) and terahertz communications with significantly tight antenna spacing in future. The received signals at UE-1 and UE-2 are defined as y_1 and y_2 , respectively, and can be expressed as

$$\begin{bmatrix} y_1 \\ y_2 \end{bmatrix} = \mathbf{H}^{\text{eff}} \begin{bmatrix} \sqrt{\alpha P} s_1 \\ \sqrt{(1-\alpha)P} s_2 \end{bmatrix} + \begin{bmatrix} w_1 \\ w_2 \end{bmatrix}, \quad (1)$$

where P is the total transmission power and α is the transmission power allocation coefficient of NOMA. w_1 and w_2 are noise at UE-1 and UE-2, respectively. Further, the effective channel impulse response matrix \mathbf{H}^{eff} can be described in detail as [13], [17]

$$\mathbf{H}^{\text{eff}} = \begin{bmatrix} h_{11} & h_{12} \\ h_{21} & h_{22} \end{bmatrix} \quad (2)$$

$$= \begin{bmatrix} \vec{p}_{UE,1}^T \mathbf{H}_{11} \vec{p}_{Tx,1} & \vec{p}_{UE,1}^T \mathbf{H}_{12} \vec{p}_{Tx,2} \\ \vec{p}_{UE,2}^T \mathbf{H}_{21} \vec{p}_{Tx,1} & \vec{p}_{UE,2}^T \mathbf{H}_{22} \vec{p}_{Tx,2} \end{bmatrix}, \quad (3)$$

where the operation $(\cdot)^T$ is the transpose of a given vector or matrix, and \mathbf{H}_{ij} is called polarization-basis matrix with the following description.

$$\mathbf{H}_{ij} = \begin{bmatrix} h_{ij}^{\text{vv}} & h_{ij}^{\text{vh}} \\ h_{ij}^{\text{hv}} & h_{ij}^{\text{hh}} \end{bmatrix}, \quad (4)$$

where h_{ij}^{xy} with $x \in \{v, h\}$; $y \in \{v, h\}$ is the XY-channel impulse response from the Y-polarization Tx antenna to the X-polarization Rx antenna. Lastly, $\vec{p}_{Tx,j}$ and $\vec{p}_{UE,i}$ are, respectively, the Tx-polarization vector at the j th Tx antenna of the gNB and the Rx-polarization vector at the antenna of UE- i Rx, and they are expressed as

$$\vec{p}_{Tx,j} = \begin{bmatrix} p_{Tx,j}^{\text{v}} \\ p_{Tx,j}^{\text{h}} \end{bmatrix} = \begin{bmatrix} \cos \theta_j \\ \sin \theta_j \end{bmatrix}, \quad (5)$$

$$\vec{p}_{UE,i} = \begin{bmatrix} p_{UE,i}^{\text{v}} \\ p_{UE,i}^{\text{h}} \end{bmatrix} = \begin{bmatrix} \cos \theta_i \\ \sin \theta_i \end{bmatrix}. \quad (6)$$

Here, we call the angles θ_j and θ_i Tx- and Rx-polarization angles, respectively. It is noteworthy that Tx- and Rx-polarization vectors are unit vectors so that the overall signal power is preserved [13], [17].

III. POLARIZATION RECONFIGURABLE NOMA (PR-NOMA) WITH DYNAMIC ORDERED SIC

The novel paradigm in PR-NOMA is that the proposed scheme realizes SIC at not only UE-1 but also UE-2 via exploiting polarization reconfigurable antenna elements at the gNB and UEs. This section describes the theoretical analyses and derivations of dynamic ordered SIC and sum/individual channel capacity.

A. Dynamic Ordered SIC

From (1) – (3), the received signals, y_1 at UE-1 and y_2 at UE-2 are, respectively,

$$y_1 = h_{11} \sqrt{\alpha P} s_1 + h_{12} \sqrt{(1-\alpha)P} s_2 + w_1, \quad (7)$$

$$y_2 = h_{21} \sqrt{\alpha P} s_1 + h_{22} \sqrt{(1-\alpha)P} s_2 + w_2. \quad (8)$$

The first term including s_1 and the second term including s_2 in (7) are, respectively, the desired signal and interfering

signal components; the conventional NOMA can eliminate the latter based on the SIC at UE-1. On the other hand, s_2 is designated for UE-2, and the first term including s_1 in (8) is the interfering signal component at UE-2. In conventional NOMA, the received interfering signal power $P_{1,UE2}$ is lower than the received desired signal power $P_{2,UE2}$ at UE-2, as portrayed at the left side of Fig. 2. Hence, UE-2 cannot apply SIC to eliminate interfering signal, but directly decode s_2 , accounting for the interfering signal.

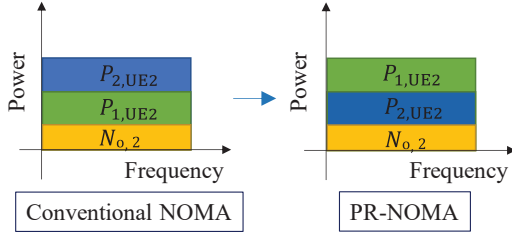


Fig. 2. Pursuit of PR-NOMA at UE-2: dynamic ordered SIC

In contrast, PR-NOMA pursues dynamic ordered SIC, i.e., the decoding order at UE-1 is different from that of UE-2. While s_2 component has the higher received signal power than s_1 component in both (7) and (8) in conventional NOMA, PR-NOMA pursues the opposite scenario that s_1 component has the higher received signal power than s_2 component only at UE-2, and UE-1 maintains the original decoding order of SIC. This swapping of decoding order at UE-2 is depicted at the right side of Fig. 2. The dynamic ordered SIC can be accomplished via tailoring polarization of antenna elements represented by the associated polarization vectors in (3).

The dynamic ordered SIC in Fig. 2 pursues the scenario $P_{1,UE2} \geq P_{2,UE2}$, which is equivalent to the scenario where

$$\left| h_{21} \sqrt{\alpha P} s_1 \right|^2 > \left| h_{22} \sqrt{(1-\alpha) P} s_2 \right|^2. \quad (9)$$

Further, h_{21} and h_{22} in (9) can be adjusted by the associated polarization vectors based on (2) – (3). Thus, the left side of the inequality in (9) is further described as

$$\begin{aligned} & \left| h_{21} \sqrt{\alpha P} s_1 \right|^2 \\ &= \alpha P \vec{p}_{Tx,1}^T \left(\mathbf{H}_{21}^\dagger \vec{p}_{UE,2} \vec{p}_{UE,2}^T \mathbf{H}_{21} \right) \vec{p}_{Tx,1} |s_1|^2 \quad (10) \end{aligned}$$

$$= \alpha P \vec{p}_{UE,2}^T \left(\mathbf{H}_{21} \vec{p}_{Tx,1} \vec{p}_{Tx,1}^T \mathbf{H}_{21}^\dagger \right) \vec{p}_{UE,2} |s_1|^2 \quad (11)$$

Our objective is first to satisfy (9) and realize dynamic ordered SIC, i.e., apply SIC to the received signal at UE-2. In the analogous manner with [13] and [17], appropriate polarization vectors, $\vec{p}_{UE,2}$ and $\vec{p}_{Tx,1}$ are determined to maximize $|h_{21}|^2$ in (9) – (11) as

$$\begin{aligned} \vec{p}_{UE,2}^{\text{SIC}} &= \arg \max_{\vec{p}_{UE,2}} \vec{p}_{UE,2}^T \left(\mathbf{H}_{21} \vec{p}_{Tx,1} \vec{p}_{Tx,1}^T \mathbf{H}_{21}^\dagger \right) \vec{p}_{UE,2} \\ &= \vec{e}_1, \quad (12) \end{aligned}$$

$$\begin{aligned} \vec{p}_{Tx,1}^{\text{SIC}} &= \arg \max_{\vec{p}_{Tx,1}} \vec{p}_{Tx,1}^T \left(\mathbf{H}_{21}^\dagger \vec{p}_{UE,2} \vec{p}_{UE,2}^T \mathbf{H}_{21} \right) \vec{p}_{Tx,1} \\ &= \vec{e}_2, \quad (13) \end{aligned}$$

where \vec{e}_1 and \vec{e}_2 are eigenvectors corresponding to the maximum eigenvalues of $\mathbf{H}_{21} \vec{p}_{Tx,1} \vec{p}_{Tx,1}^T \mathbf{H}_{21}^\dagger$ in (12) and $\mathbf{H}_{21}^\dagger \vec{p}_{UE,2} \vec{p}_{UE,2}^T \mathbf{H}_{21}$ in (13), respectively.

In the analogous manner with (9) at UE-2, the following condition should be satisfied by UE-1.

$$\left| h_{12} \sqrt{(1-\alpha) P} s_2 \right|^2 > \left| h_{11} \sqrt{\alpha P} s_1 \right|^2. \quad (14)$$

It is worth emphasizing that the transmission power allocation coefficient α is not always less than 0.5 in PR-NOMA as will be illustrated in Section IV. Therefore, it is required to determine polarization vectors considering the feasibility of SIC even at the near user, UE-1. Based on (14), appropriate polarization vectors, $\vec{p}_{UE,1}$ and $\vec{p}_{Tx,2}$ are determined to maximize $|h_{12}|^2$ for the feasibility of SIC at UE-1, in the analogous fashion with the aspect UE-2 described above. That is,

$$\begin{aligned} \vec{p}_{UE,1}^{\text{SIC}} &= \arg \max_{\vec{p}_{UE,1}} \vec{p}_{UE,1}^T \left(\mathbf{H}_{12} \vec{p}_{Tx,2} \vec{p}_{Tx,2}^T \mathbf{H}_{12}^\dagger \right) \vec{p}_{UE,1} \\ &= \vec{e}_3, \quad (15) \end{aligned}$$

$$\begin{aligned} \vec{p}_{Tx,2}^{\text{SIC}} &= \arg \max_{\vec{p}_{Tx,2}} \vec{p}_{Tx,2}^T \left(\mathbf{H}_{12}^\dagger \vec{p}_{UE,1} \vec{p}_{UE,1}^T \mathbf{H}_{12} \right) \vec{p}_{Tx,2} \\ &= \vec{e}_4, \quad (16) \end{aligned}$$

where \vec{e}_3 and \vec{e}_4 are eigenvectors corresponding to the maximum eigenvalues of $\mathbf{H}_{12} \vec{p}_{Tx,2} \vec{p}_{Tx,2}^T \mathbf{H}_{12}^\dagger$ in (15) and $\mathbf{H}_{12}^\dagger \vec{p}_{UE,1} \vec{p}_{UE,1}^T \mathbf{H}_{12}$ in (16), respectively.

B. Sum and Individual Channel Capacity in PR-NOMA

The conventional NOMA applies SIC to UE-1; meanwhile, UE-2 cannot fulfill SIC since the reception power of the desired signal s_2 is greater than that of the interfering signal s_1 in (8). In contrast, the proposed PR-NOMA with dynamic ordered SIC enables UE-2 to fulfill SIC and eliminate the interfering signal. Thus, the individual channel capacity of UE-2 is significantly improved; in turn, the sum channel capacity is also remarkably increased. This section provides the theoretical analysis of individual and sum channel capacity in PR-NOMA.

In the scenario of the conventional NOMA, the individual channel capacity of UE-1 and UE-2, C_1^{NOMA} and C_2^{NOMA} , respectively, are expressed as

$$C_1^{\text{NOMA}} = \log_2 \left(1 + \frac{\alpha P |\vec{p}_{UE,1}^T \mathbf{H}_{11} \vec{p}_{Tx,1}|^2 |s_1|^2}{N_{o,1}} \right), \quad (17)$$

$$C_2^{\text{NOMA}} = \log_2 \left(1 + \frac{(1-\alpha) P |\vec{p}_{UE,2}^T \mathbf{H}_{22} \vec{p}_{Tx,2}|^2 |s_2|^2}{\alpha P |\vec{p}_{UE,2}^T \mathbf{H}_{21} \vec{p}_{Tx,1}|^2 |s_1|^2 + N_{o,2}} \right). \quad (18)$$

On the other hand, in PR-NOMA, the individual channel capacity of UE-1 and UE-2, $C_1^{\text{PR-NOMA}}$ and $C_2^{\text{PR-NOMA}}$, respectively, are

$$C_1^{\text{PR-NOMA}} = \log_2 \left(1 + \frac{\alpha P |\vec{p}_{UE,1}^T \mathbf{H}_{11} \vec{p}_{Tx,1}|^2 |s_1|^2}{N_{o,1}} \right), \quad (19)$$

$$C_2^{\text{PR-NOMA}} = \log_2 \left(1 + \frac{(1-\alpha) P |\vec{p}_{UE,2}^T \mathbf{H}_{22} \vec{p}_{Tx,2}|^2 |s_2|^2}{N_{o,2}} \right). \quad (20)$$

Sum channel capacity of the conventional NOMA, $C_{\text{sum}}^{\text{NOMA}}$ and that of PR-NOMA, $C_{\text{sum}}^{\text{PR-NOMA}}$ are expressed as

$$C_{\text{sum}}^{\text{NOMA}} = C_1^{\text{NOMA}} + C_2^{\text{NOMA}}, \quad (21)$$

$$C_{\text{sum}}^{\text{PR-NOMA}} = C_1^{\text{PR-NOMA}} + C_2^{\text{PR-NOMA}}. \quad (22)$$

In comparison of $C_2^{\text{PR-NOMA}}$ in (20) to C_2^{NOMA} in (18), we can expect the significant increase of individual and sum channel capacity in PR-NOMA, and simulation results validates it in Section IV. It is worth emphasizing that the described enhancement of sum and individual channel capacity in PR-NOMA is resulted from determination of polarization vectors to satisfy conditions in (9) and (14) for realizing dynamic ordered SIC.

C. Optimal Transmission Power Allocation Coefficient

The individual channel capacity at UE-2 of PR-NOMA, $C_2^{\text{PR-NOMA}}$ in (20) is a concave function since the interfering signal component can be eliminated by dynamic ordered SIC. Consequently, the sum channel capacity of PR-NOMA, $C_{\text{sum}}^{\text{PR-NOMA}}$ in (22) is also concave. For this reason, Lagrangian optimization can provide the optimal transmission power allocation coefficient of PR-NOMA, α^{opt} , due to the impact of dynamic ordered SIC on the formula of channel capacity.

For the simplicity in (19) – (20), β and γ are defined as

$$\beta \triangleq P |\vec{P}_{\text{UE},1}^T \mathbf{H}_{11} \vec{P}_{\text{Tx},1}|^2 |s_1|^2, \quad (23)$$

$$\gamma \triangleq P |\vec{P}_{\text{UE},2}^T \mathbf{H}_{22} \vec{P}_{\text{Tx},2}|^2 |s_2|^2. \quad (24)$$

Then, utilizing β and γ ,

$$C_{\text{sum}}^{\text{PR-NOMA}} = \log_2 \left(1 + \frac{\alpha\beta}{N_{o,1}} \right) + \log_2 \left(1 + \frac{(1-\alpha)\gamma}{N_{o,2}} \right). \quad (25)$$

In the analogous manner with Lagrangian optimization in water-filling power allocation, the optimal transmission power allocation coefficient, α^{opt} can be derived as [24],

$$\alpha^{\text{opt}} = \frac{1}{2} \left(1 + \frac{N_{o,2}}{\gamma} - \frac{N_{o,1}}{\beta} \right). \quad (26)$$

The determined polarization vectors in Section III-A along with the polarization-basis matrices in Section II can yield α^{opt} , and it is verified in overall simulations.

IV. NUMERICAL EVALUATION AND RESULTS

This section provides comprehensive simulation results to validate significantly enhanced performance of PR-NOMA in terms of sum channel capacity along with individual channel capacity, comparing to that of the conventional NOMA. The statistical Gaussian fading channel model is adopted to exhibit remarkable increase in channel capacity in a statistical sense. On the other hand, deterministic channel models are also utilized, demonstrating the characteristics of the PR-NOMA system.

The range of the transmission power allocation coefficient, α for successful dynamic ordered SIC, is portrayed in Fig. 3, considering two distinct deterministic channels. The range of α satisfying (9) and (14) can be expressed as $\alpha_{\text{lb}} \leq \alpha \leq \alpha_{\text{ub}}$,

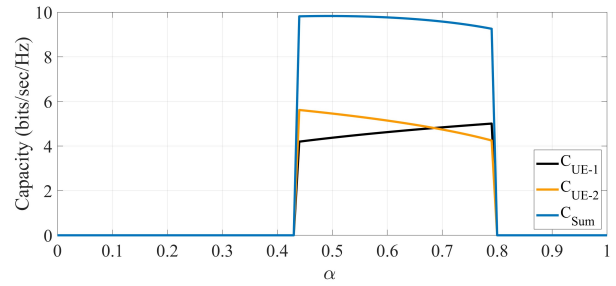


Fig. 3. Two deterministic channels with different intervals of α satisfying dynamic ordered SIC constraints.

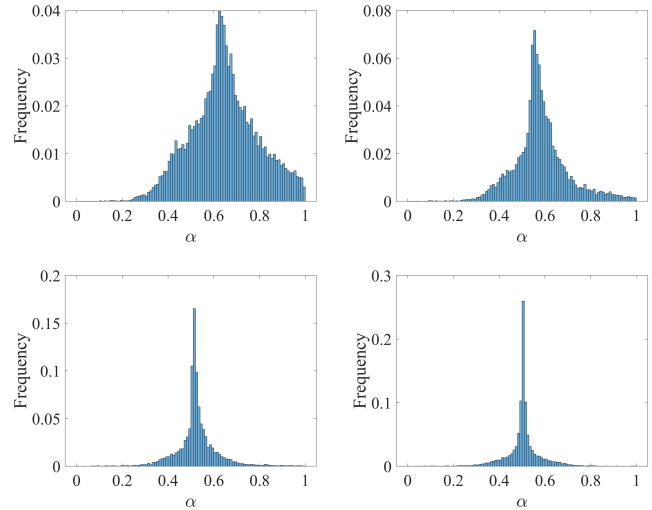


Fig. 4. The histogram of α^{opt} in PR-NOMA for different values of UE2 SNR: 3 dB (top left), 8 dB (top right), 15 dB (bottom left) and 20 dB (bottom right).

where the lower bound, α_{lb} and the upper bound, α_{ub} are indicated by the left and right bounds, respectively, in Fig. 3. For $\alpha < \alpha_{\text{lb}}$, only UE-1 can fulfill SIC; meanwhile, for $\alpha > \alpha_{\text{ub}}$ only UE-2 can apply SIC. These intervals are dependent on channel realizations and the determined polarization vectors based on Section III-A.

The distribution of the optimal transmission power allocation coefficient, α^{opt} in (26) for the proposed PR-NOMA is demonstrated in Fig. 4. It is noteworthy that α^{opt} of PR-NOMA varies substantially over channel realizations in Fig. 4. Further, the SNR difference between UE-1 and UE-2 has a crucial impact on the distribution. In contrast, conventional NOMA has almost the constant α^{opt} . The probability that $\alpha^{\text{opt}} = 0$ increases as the SNR of UE-2 increases; it approaches 50 % when the SNR of UE-2 approaches that of UE-1, 20 dB. That is, when UE-1 and UE-2 have the same SNR, 20 dB, allocating total transmission power to UE-2 maximizes sum channel capacity with 50 % probability.

Furthermore, in Fig. 4, beginning with 3 dB SNR of UE-2, α^{opt} is frequently greater than 0.5. That is, more transmission power is allocated to UE-1, the near user. When UE-1 and UE-2 have the same SNR, 20 dB, the distribution becomes symmetric with respect to $\alpha = 0.5$, i.e., equal transmission

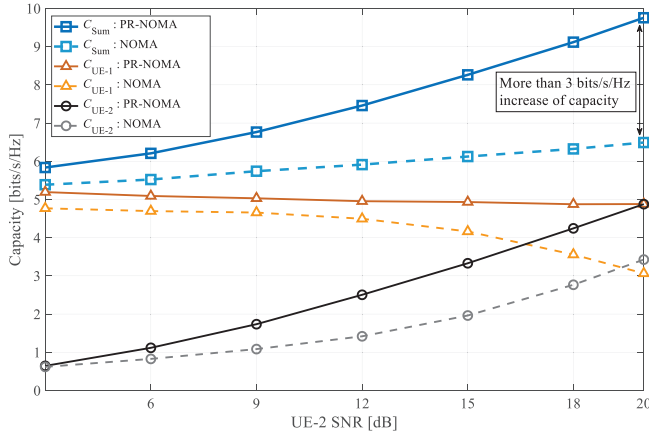


Fig. 5. Individual user and sum channel capacity of the proposed PR-NOMA scheme compared to conventional NOMA scheme as a function of UE-2 SNR. UE-1 SNR is fixed to 20 dB.

power allocation. It is feasible to have sufficient reception power difference between the desired signal and the interfering signal, utilizing polarization reconfigurable antennas even with $\alpha^{\text{opt}} = 0.5$.

The individual and sum channel capacity in PR-NOMA and conventional NOMA, are portrayed and compared to each other in Fig. 5. It is worth emphasizing that the sum and individual channel capacity of PR-NOMA remarkably outperforms that of conventional NOMA, in particular, as the distance from the gNB to UE-1 and UE-2 becomes similar, i.e., SNR of UE-2 increases to be 20 dB. The capacity curves for 0 to 20 dB SNR regime of UE-2 are resulted from statistical realizations of additive white Gaussian noise (AWGN) channels; meanwhile, the SNR of UE-1 is fixed to be 20 dB.

It is noteworthy that the sum channel capacity of PR-NOMA remarkably outperforms that of conventional NOMA by more than 3 bits/s/Hz at 20 dB SNR of UE-2. The novel scheme of PR-NOMA can apply dynamic ordered SIC, and performs SIC at not only UE-1 but also UE-2 even when both UEs have the same SNR, i.e., 20 dB. Further, UE-1 maintains satisfactory individual capacity, i.e., $C_{\text{UE-1}}$ in PR-NOMA; while $C_{\text{UE-1}}$ of conventional NOMA substantially decreases in high SNR regime of UE-2, e.g., 15 to 20 dB as the cost of increasing the individual capacity of UE-2, $C_{\text{UE-2}}$.

V. CONCLUSION

A novel scheme of PR-NOMA with dynamic ordered SIC is proposed. The comprehensive simulations support the benefit of PR-NOMA, which significantly outperforms conventional NOMA. PR-NOMA can apply SIC at both users even when they have the same SNR, and it exhibits more than 3 bits/sec/Hz improvement of sum channel capacity in the statistical channel model. The range of transmission power allocation coefficient in PR-NOMA is far wider than that in conventional NOMA; therefore, PR-NOMA supports the communication system more flexibly for the change of wireless channels than conventional NOMA.

REFERENCES

- [1] Z. Ding, F. Adachi, and H. V. Poor, "The application of MIMO to non-orthogonal multiple access," *IEEE Trans. Wireless Commun.*, vol. 15, no. 1, pp. 537–552, 2016.
- [2] Z. Ding, Z. Yang, P. Fan, and H. V. Poor, "On the performance of non-orthogonal multiple access in 5G systems with randomly deployed users," *IEEE Signal Proc. Lett.*, vol. 21, no. 12, pp. 1501–1505, 2014.
- [3] A. Benjebbour, A. Li, Y. Saito, Y. Kishiyama, A. Harada, and T. Nakamura, "System-level performance of downlink NOMA for future LTE enhancements," *IEEE Globecom Workshops*, pp. 66–70, 2013.
- [4] A. Benjebbour, A. Li, Y. Kishiyama, H. Jiang, and T. Nakamura, "System-level performance of downlink NOMA combined with SU-MIMO for future LTE enhancements," *IEEE Globecom Workshops*, pp. 706–710, 2014.
- [5] Y. Saito, Y. Kishiyama, A. Benjebbour, T. Nakamura, A. Li, and K. Higuchi, "Non-orthogonal multiple access (NOMA) for cellular future radio access," in *Proc. IEEE Veh. Technol. Conf.*, 2013, pp. 1–5.
- [6] Z. Ding, P. Fan, and H. V. Poor, "Impact of user pairing on 5G nonorthogonal multiple-access downlink transmissions," *IEEE Trans. Veh. Technol.*, vol. 65, no. 8, pp. 6010–6023, 2016.
- [7] F. Fang, H. Zhang, J. Cheng, S. Roy, and V. C. M. Leung, "Joint user scheduling and power allocation optimization for energy-efficient NOMA systems with imperfect CSI," *IEEE J. Sel. Areas Commun.*, vol. 35, no. 12, pp. 2874–2885, 2017.
- [8] C.-L. Wang, J.-Y. Chen, and Y.-J. Chen, "Power allocation for a downlink non-orthogonal multiple access system," *IEEE Commun. Lett.*, vol. 5, no. 5, pp. 532–535, 2016.
- [9] Z. Yang, W. Xu, C. Pan, Y. Pan, and M. Chen, "On the optimality of power allocation for NOMA downlinks with individual QoS constraints," *IEEE Commun. Lett.*, vol. 21, no. 7, pp. 1649–1652, 2017.
- [10] J. Choi, "Power allocation for max-sum rate and max-min rate proportional fairness in NOMA," *IEEE Commun. Lett.*, vol. 20, no. 10, pp. 2055–2058, 2016.
- [11] I.-H. Lee and J.-B. Kim, "Average symbol error rate analysis for non-orthogonal multiple access with m -ary QAM signals in Rayleigh fading channels," *IEEE Commun. Lett.*, vol. 23, no. 8, pp. 1328–1331, 2019.
- [12] P. Oh and S. Kwon, "Multipolarization superposition beamforming: Novel scheme of transmit power allocation and subcarrier assignment," *IEEE Trans. Wireless Commun.*, vol. 22, no. 1, pp. 658–670, 2023.
- [13] P. S. Oh, S. S. Kwon, and A. F. Molisch, "Antenna selection in polarization reconfigurable MIMO (PR-MIMO) communication systems," *CoRR*, arXiv, pp. 1–13, 2021.
- [14] K. Satyanarayana, T. Ivanescu, M. El-Hajjar, P. Kuo, A. Mourad, and L. Hanzo, "Hybrid beamforming design for dual-polarised millimetre wave MIMO systems," *IET Electronics Lett.*, vol. 54, no. 22, pp. 1257–1258, 2018.
- [15] O. Jo, J. Kim, J. Yoon, D. Choi, and W. Hong, "Exploitation of dual-polarization diversity for 5G millimeter-wave MIMO beamforming systems," *IEEE Trans. Antennas Propag.*, vol. 65, no. 12, pp. 6646–6655, Dec. 2017.
- [16] X. Zhang, B. Zhang, and D. Guo, "Performance of poly-polarization multiplexing in narrow-band wireless communication aided by pre-compensation and multi-notch OPFs," *IEEE Wireless Commun. Lett.*, vol. 6, no. 4, pp. 478–481, Aug. 2017.
- [17] S.-C. Kwon and A. F. Molisch, "Capacity maximization with polarization-agile antennas in the MIMO communication system," *Proc. IEEE Global Telecommun. Conf.*, pp. 1–6, Dec. 2015.
- [18] S.-C. Kwon, "Optimal power and polarization for the capacity of polarization division multiple access channels," *Proc. IEEE Global Telecommun. Conf.*, pp. 1–5, Dec. 2014.
- [19] S.-C. Kwon and G. Stüber, "Polarization division multiple access on NLoS wide-band wireless fading channels," *IEEE Trans. Wireless Commun.*, vol. 13, no. 7, pp. 3726–3737, Jul. 2014.
- [20] J. Jootar, J.-F. Diouris, and J. Zeidler, "Performance of polarization diversity in correlated Nakagami-m fading channels," *IEEE Trans. Veh. Technol.*, vol. 55, no. 1, pp. 128–136, 2006.
- [21] S.-C. Kwon and G. L. Stüber, "Geometrical theory of channel depolarization," *IEEE Trans. Veh. Technol.*, vol. 60, no. 8, pp. 3542–3556, Oct. 2011.
- [22] S.-C. Kwon, G. Stüber, A. López, and J. Papapolymerou, "Geometrically based statistical model for polarized body-area-network channels," *IEEE Trans. Veh. Technol.*, vol. 62, no. 8, pp. 3518–3530, Oct. 2013.
- [23] A. Molisch and M. Win, "MIMO systems with antenna selection," *IEEE Microwave Mag.*, vol. 5, no. 1, pp. 46–56, Mar. 2004.
- [24] D. Tse and P. Viswanath, *Fundamentals of Wireless Communication*, 1st ed. Cambridge, 2005.